Research Article | Open Access

Greenverse Science

Wang *et al. Greenverse Sci.* **2026**, *1*, 9 **DOI:**10.20517/greenvsci.2026.08

Promoting effect of hydroxyl groups on the CO-SCR activity of Ir-Mo bimetallic catalysts under O_2 and SO_2

Yixi Wang[1], Xiubiao Ma[1,2], Huixian Liu[3], Yujie Yuan[1,4], Yang Yang[1], Yaping Zhang[2], Wenqing Xu[1,*], Tingyu Zhu[1]

Keywords:
NO_x removal, selective catalytic reduction, Ir-Mo bimetallic clusters, hydroxyl groups, promotion mechanism of SO_2

Citation: Wang, Y.; Ma, X.; Liu, H.; Yuan, Y.; Yang, Y.; Zhang, Y.; Xu, W.; Zhu, T. Promoting effect of hydroxyl groups on the CO-SCR activity of Ir-Mo bimetallic catalysts under O_2 and SO_2. *Greenverse Sci.* **2026**, *1*, 9. https://dx.doi.org/10.20517/greenvsci.2026.08

Received: 18 Mar 2026 **First Decision:** 13 Apr 2026 **Revised:** 22 May 2026 **Accepted:** 25 May 2026 **Published:** 16 Jun 2026

Academic Editor: Dengsong Zhang **Copy Editor:** Xing-Yue Zhang **Production Editor:** Xing-Yue Zhang

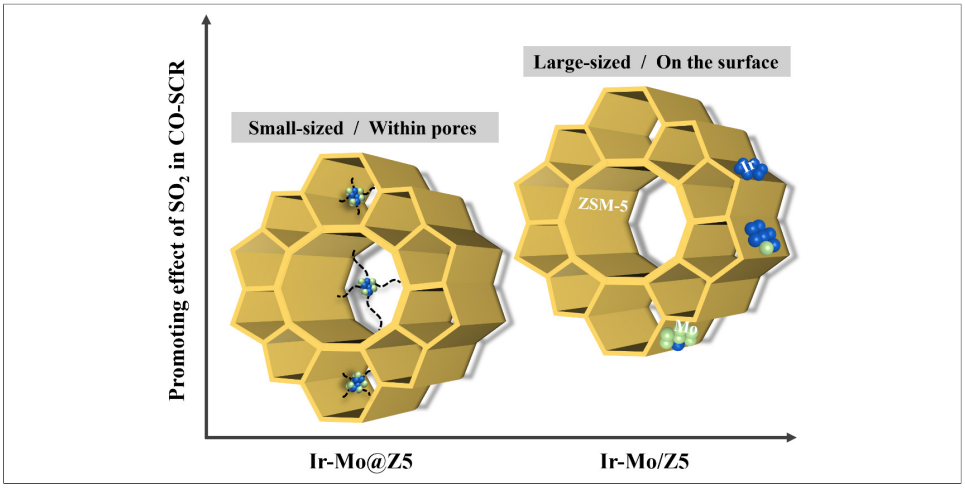

Abstract

The incorporation of promoters to form bimetallic clusters is a feasible strategy for boosting catalyst performance in the selective catalytic reduction of nitrogen oxides (NO_x) by carbon monoxide (CO) (CO-SCR); however, developing bimetallic catalysts suitable for complex flue gas conditions remains challenging. This study reports a highly dispersed, sub-nanometer iridium-molybdenum (Ir-Mo) cluster catalyst predominantly confined within ZSM-5 (MFI-type zeolite) crystals (denoted as Ir-Mo@Z5), in which hydroxyl groups (-OH) serve as active sites, thereby preserving high catalytic performance under oxygen (O_2)- and sulfur dioxide (SO_2)-containing conditions. Remarkably, this catalyst achieves ~62.4% NO_x conversion at 275 °C in the presence of 5% O_2 and 200 ppm SO_2. The crucial role of the -OH groups is revealed by comparison with an Ir-Mo/Z5 catalyst prepared by conventional impregnation. On the one hand, the -OH groups are generally occupied by Ir species, thereby reducing the extent of CO oxidation and promoting NO reduction by CO. On the other hand, the oxidation of SO_2 on the catalyst and the resulting

[1]CAS Key Laboratory of Green Process and Engineering, Institute of Process Engineering, Chinese Academy of Sciences, Beijing 100190, China.
[2]Key Laboratory of Energy Thermal Conversion and Control, School of Energy and Environment, Southeast University, Nanjing 210096, Jiangsu, China.
[3]Beijing Municipal Research Institute of Eco-Environmental Protection, Beijing 100037, China.
[4]School of Chemistry and Chemical Engineering, North University of China, Taiyuan 030051, Shanxi, China.

[*]**Correspondence to:** Prof. Wenqing Xu, CAS Key Laboratory of Green Process and Engineering, Institute of Process Engineering, Chinese Academy of Sciences, Beijing 100190, China. E-mail: wqxu@ipe.ac.cn

consumption of -OH groups, especially the bridging silanol-aluminum group (Si-OH-Al), constitute the intrinsic mechanism that reduces the nitrate-mediated "ineffective reaction pathway" in the presence of O_2. This work elucidates how the structural state of bimetallic clusters influences the SO_2-promoted -OH mechanism, guiding the rational design of high-performance bimetallic CO-SCR catalysts tailored for complex reaction conditions.

INTRODUCTION

Nitrogen oxides (NO_x), primarily nitric oxide (NO), nitrous oxide (N_2O), and nitrogen dioxide (NO_2), are major air pollutants that contribute to photochemical smog and acid rain and pose serious threats to human health[1,2]. Although selective catalytic reduction (SCR) technology using ammonia (NH_3) as a reducing agent (NH_3-SCR) has been widely applied for the removal of stationary-source NO_x, it suffers from drawbacks such as NH_3 slip and the high cost of NH_3 storage and transportation[3]. The CO-SCR technology, using carbon monoxide (CO) instead of NH_3 as a reducing agent, has become a research hotspot in recent years, as CO is a byproduct of the incomplete combustion of carbon-based fuels and is present at high concentrations in industrial flue gas[4-6]. This technology is of great significance for the coordinated control of NO_x and CO emissions simultaneously.

However, the activity of most CO-SCR catalysts is limited by the presence of oxygen (O_2), as CO is more likely to be oxidized than participate in NO_x reduction. Compared to other catalysts, iridium (Ir)-based catalysts exhibit superior performance in O_2-containing environments and have been widely studied[7,8]. Typically, Ir^0 is considered the main active site because the electrons are transferred from Ir^0 to the antibonding π orbital of NO, thereby weakening the N–O bond[9]. Furthermore, $Ir^{\delta+}$ serves as a charge-transfer bridge, accepting electrons from the carbon (C) atom of CO and facilitating redox cycling[10]. Our previous research has confirmed that an Ir-based catalyst encapsulated in Zeolite Socony Mobil-5 (ZSM; Ir@ZSM-5) is more effective[11], as Ir and $Ir^{\delta+}$ are more likely to reach dynamic equilibrium in the presence of O_2 and SO_2 due to the micropore confinement.

Recently, an increasing number of studies have shown that adding promoters to form bimetallic clusters enhances the performance of CO-SCR catalysts. Ji *et al.*[12] demonstrated that the electronegativity difference between Ir and tungsten (W) promotes electron transfer, thereby improving CO-SCR activity. Isolated Ir single atoms and Ir-W intermetallic nanoparticles coexist on ordered mesoporous SiO_2 (KIT-6), enabling complete NO conversion to nitrogen (N_2) at 250 °C under 1% O_2. Similarly, Wang *et al.*[13] found that highly dispersed Ir and tungsten oxide (WO_3) species facilitated strong Ir-W interactions, resulting in more exposed Ir^0 and Ir-WO_{3-x} active sites and enhancing the adsorption and dissociation of NO. Takahashi *et al.*[14] also proposed that Ir-WO_x species ($2.92 \leq x \leq 3$) on Ir/WO_3-SiO_2 promote NO dissociation. However, these studies remain limited to bimetallic clusters supported on the surface. Research on enhancing the CO-SCR performance of bimetallic clusters via zeolite micropore confinement remains scarce.

Herein, we report that iridium-molybdenum (Ir-Mo) bimetallic clusters encapsulated within ZSM-5 achieve highly efficient CO-SCR in the presence of oxygen (O_2) and sulfur dioxide (SO_2). Mo, which belongs to the same group as W, is also a commonly used active component for NO adsorption and dissociation in SCR catalysts[15]. Previous studies have shown that smaller molybdenum trioxide (MoO_3) particles interact more readily with Brønsted acid sites on the surface of ZSM-5 to form Mo-O-Al species, resulting in a favorable phase structure of the Mo/ZSM-5 catalyst for NO reduction[16,17]. In addition, Xie *et al.*[18] reported that preferential anchoring of Mo atoms at terminal hydroxyl (-OH) groups on the support promotes the aggregation of other low-loading noble metal atoms into highly concentrated electron-rich species. Similarly, Fu *et al.*[19] confirmed that the addition of Mo is beneficial for reducing the oxidation state of Ir in the Ir/TiO_2 catalyst.

In this work, we employed a one-step synthesis to prepare an Ir-Mo@ZSM-5 catalyst, in which Ir-Mo bimetallic clusters were spatially confined within the

ordered ZSM-5 framework. This spatial confinement balances the contents of Ir^0 and $Ir^{\delta+}$ species, leading to superior NO_x conversion performance. The Ir-Mo@ZSM-5 catalyst achieved a NO_x conversion of approximately 62.4% at 275 °C under simulated industrial flue gas conditions (400 ppm NO, 8,000 ppm CO, 5% O_2, and 200 ppm SO_2). This study highlights the effectiveness of zeolite micropore confinement in enhancing the CO-SCR performance of bimetallic clusters. Further, it reveals, through systematic investigation of hydroxyl groups, that the structural state of the bimetallic clusters governs the SO_2 promotion mechanism, providing valuable insights for the rational design of highly efficient CO-SCR catalysts.

EXPERIMENT

Catalyst preparation

Tetrapropylammonium bromide (TPABr, 98%), silica sol (20%-40%), sodium aluminate ($NaAlO_2$, analytical reagent), and sodium hydroxide (NaOH, 96%) were purchased from Shanghai Macklin Biochemical Co., Ltd. Hexachloroiridic acid hydrate ($H_2Cl_6Ir{\cdot}xH_2O$, 36%), ammonium molybdate [$(NH_4)_6Mo_7O_{24}{\cdot}4H_2O$], ethylenediamine (EDA, 99.5%), and tetraethylenepentamine (TEPA, technical grade) were purchased from Shanghai Aladdin Biochemical Technology Co., Ltd. Unless otherwise specified, all chemicals were of analytical grade and used as received without further purification.

TPABr, silica sol, $NaAlO_2$, and NaOH were used for preparing ZSM-5 (hereinafter referred to as Z5). An improved ligand-protected one-step synthesis strategy was used to obtain ZSM-5-encaged Ir-Mo bimetallic clusters, denoted as Ir-Mo@Z5. Ir-Mo/Z5 catalysts were prepared by the impregnation method with the same metal loading for comparison. The symbols "@" and "/" are used to distinguish catalysts prepared via encapsulation within zeolite frameworks and surface-supported configurations, respectively. Before evaluating catalytic performance, the synthesized Ir-Mo@Z5 and Ir-Mo/Z5 catalysts were pretreated in 5% hydrogen/argon (H_2/Ar) at 200 °C for 30 min. The detailed synthetic method is provided in the Supplementary Materials. A schematic diagram of Ir-Mo@Z5 catalyst preparation is shown in Supplementary Figure 1.

Catalytic performance evaluation and catalyst characterization

The activity measurements of CO-SCR at atmospheric pressure were conducted in a quartz tubular continuous-flow reactor (inner diameter = 6 mm) using 40-60 mesh catalyst particles. The total flow rate of the simulated reactant gas was 100 $mL{\cdot}min^{-1}$ with a gas hourly space velocity (GHSV) of 16,000 h^{-1}. The gas composition contained 400 ppm NO, 8,000 ppm CO, 5% O_2, 200 ppm SO_2, and N_2 as the balance gas. Concentrations of CO and NO_x were analyzed in real time using an online Fourier transform infrared (FTIR) spectrometer equipped with a deuterated triglycine sulfate (DTGS) detector. The conversion and selectivity were calculated as below[20]:

$$X_{NO_x} = \left[\frac{NO(in)-NO(out)-N_2O(out)-NO_2(out)}{NO(in)}\right] \times 100\%, \quad (1)$$

$$X_{NO} = \left[\frac{NO(in)-NO(out)}{NO(in)}\right] \times 100\%, \quad (2)$$

$$X_{CO} = \left[\frac{CO(in)-CO(out)}{CO(in)}\right] \times 100\%, \quad (3)$$

$$S_{N_2} = \left[\frac{NO(in)-NO(out)-2N_2O(out)-NO_2(out)}{NO(in)-NO(out)}\right] \times 100\%, \quad (4)$$

$$S_{N_2O} = \left[\frac{2N_2O(out)}{NO(in)-NO(out)}\right] \times 100\%, \quad (5)$$

$$S_{NO_2} = \left[\frac{NO_2(out)}{NO(in)-NO(out)}\right] \times 100\%. \quad (6)$$

Detailed information on catalyst characterizations is provided in the Supplementary Materials.

RESULTS AND DISCUSSION

CO-SCR performance

The CO-SCR performance of Ir-Mo@Z5 and Ir-Mo/Z5 catalysts under typical industrial flue gas conditions was evaluated within the temperature range of 150-400 °C. The results are presented in Figure 1. As shown in Figure 1A, the NO conversion of both samples follows a volcano curve, with or without SO_2 introduction, consistent with recent reports in the literature[13,21]. It is worth noting that after SO_2 injection, the NO conversion of Ir-Mo/Z5 increased significantly, whereas that of Ir-Mo@Z5 decreased slightly. Comparison of the NO conversion of Ir-Mo@Z5 with that of several high-performance bimetallic catalysts reported in the literature [Supplementary Table 1] shows that Ir-Mo@Z5 exhibits superior catalytic performance under comparable

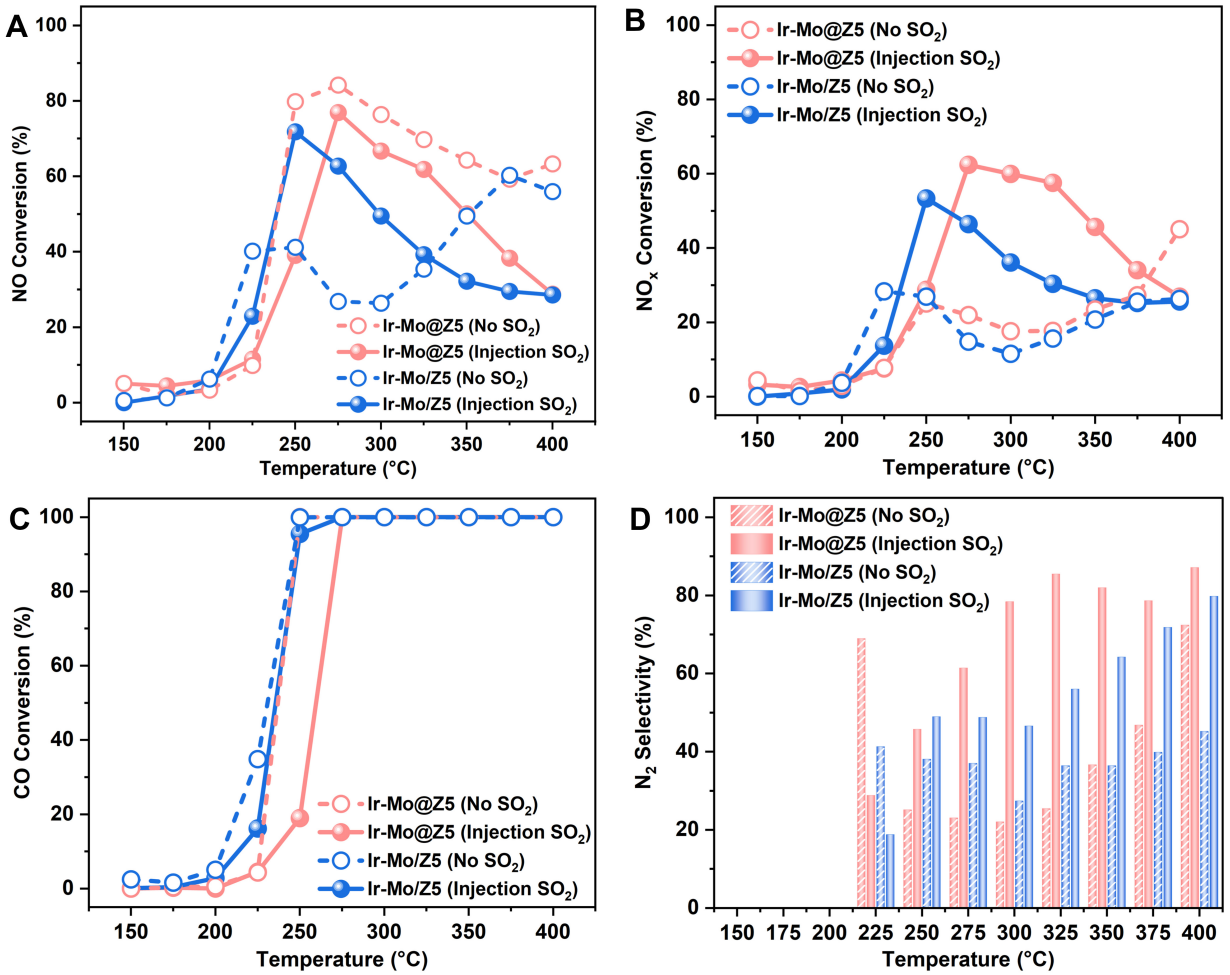

Figure 1. CO-SCR performance of Ir-Mo@Z5 and Ir-Mo/Z5 catalysts: (A) NO conversion, (B) NO_x conversion, (C) CO conversion, and (D) N_2 selectivity. Reaction conditions: [NO] = 400 ppm, [CO] = 8,000 ppm, [O_2] = 5%, [SO_2] = 200 ppm (when used), GHSV = 16,000 h^{-1}. SCR: Selective catalytic reduction; GHSV: gas hourly space velocity.

reaction conditions, highlighting its advantages and potential applications in CO-SCR systems. To more accurately reflect the actual efficiency of NO reduction to N_2 and eliminate the interference from byproducts such as NO_2, NO_x conversion is presented in Figure 1B. Unlike NO conversion, NO_x conversion is synchronously promoted for both samples after SO_2 injection. The NO_x conversion of Ir-Mo@Z5 was higher than that of Ir-Mo/Z5 across the entire temperature range, reaching a maximum of 62.4%. Subsequently, the long-term catalytic stability of Ir-Mo@Z5 and Ir-Mo/Z5 was further evaluated. As shown in Supplementary Figure 2, both catalysts exhibit excellent durability during continuous reaction, demonstrating their promising potential for practical applications. Figure 1C confirms that CO achieves nearly complete conversion at the temperature where NO or NO_x conversion reaches a maximum over both catalysts, indicating that the volcano-shaped NO or NO_x conversion profile originates from preferential oxidation of CO by O_2 at elevated temperatures. In addition, Figure 1D indicates that the SO_2 injection effectively improves N_2 selectivity, and Ir-Mo@Z5 exhibits superior N_2 selectivity compared to Ir-Mo/Z5. Supplementary Figure 3 illustrates the effect of O_2 on CO-SCR performance at 275 °C. Firstly, both catalysts exhibit reduced NO_x conversion with increasing O_2 concentration. However, Ir-Mo@Z5 maintains higher activity in the absence of the SO_2 promotional effect, indicating better O_2 tolerance.

These results indicate that although SO_2 exhibits similar promotional effects on NO_x conversion over the two catalysts, the underlying mechanisms differ. Undoubtedly, SO_2 effectively improves the selective reduction of NO to N_2. As we previously reported[22],

this is attributed to the regulatory effect of SO_2 on the "ineffective reaction pathway" in the presence of O_2 with nitrate as an intermediate. More importantly, SO_2 also promotes NO adsorption on catalysts prepared by the conventional impregnation method.

Physical and chemical characterizations

Supplementary Figure 4 shows the X-ray diffraction (XRD) patterns of Ir-Mo@Z5 and Ir-Mo/Z5 catalysts. The obtained catalysts exhibited a well-ordered MFI-type zeolite structure of Z5 (PDF#44-0003)[23,24]. No distinct characteristic peaks corresponding to Ir or Mo species were detected due to the low metal loading and high dispersion[25]. The results demonstrate that the addition of EDA, TEPA, and metal precursors into the synthetic gel had a negligible effect on the crystallization of the Z5 support. N_2 adsorption-desorption isotherms of both Ir-Mo@Z5 and Ir-Mo/Z5 catalysts exhibit typical Type I behavior [Supplementary Figure 5], indicating a microporous structure with a dominant pore size of ~0.55 nm [Supplementary Figure 6]. As summarized in Supplementary Table 2, both catalysts maintain relatively high specific surface areas (~280 m^2g^{-1}), which provide abundant sites for the adsorption of CO and NO molecules. Inductively coupled plasma (ICP) analysis indicates that the Si/Al ratios of both catalysts are approximately 25. The results also reveal that the loadings of Ir and Mo are ~0.4 and 0.85 wt.%, respectively, confirming successful incorporation of Ir and Mo into the Z5 support.

According to the transmission electron microscopy (TEM) images of the catalysts [Figure 2], the well-dispersed Ir species in Ir-Mo@Z5 exhibited an average size of 1.0 nm through the one-step synthesis method. The observation that these clusters are larger than the micropore channels in Z5 (0.55 nm) can be attributed to partial collapse of neighboring micropores during metal growth[26]. In other words, the clusters are likely confined within zeolite crystals rather than within the microporous channels[27]. Combined with energy-dispersive X-ray spectroscopy (EDS) mapping results, the Mo signal completely overlaps with that of Ir, suggesting the formation of Ir-Mo bimetallic clusters[23]. In addition, Ir-Mo bimetallic clusters show clear interplanar lattice fringes of 0.23 nm, which may correspond to the Ir (111) facet, implying the favorable dispersion of Mo species on the Ir surface. Previous studies have found that the fraction of bimetallic clusters in zeolite-supported catalysts gradually increases with prolonged hydrogen (H_2) reduction time[12,28], confirming that H_2 pretreatment is beneficial for the formation of Ir-Mo bimetallic interactions. In contrast, larger bimetallic clusters (with an average size of ~8.0 nm) were unevenly distributed on the zeolite's external surface in catalysts prepared by the conventional impregnation method.

The Ir 4f X-ray photoelectron spectroscopy (XPS) spectra of Ir-Mo@Z5 and Ir-Mo/Z5 catalysts are shown in Figure 3. In Figure 3A, the Ir $4f_{7/2}$ peak centered at 61.20 eV and 62.20 eV observed for Ir-Mo@Z5, which were assigned to metallic Ir^0 and oxidized $Ir^{\delta+}$, respectively[29,30]. After peak fitting, it was found that the proportion of Ir^0 in Ir-Mo@Z5 was 52.77%, which is significantly lower than that in Ir^0 on Ir-Mo/Z5 (61.54%) [Figure 3B]. Therefore, we confirm that the ratio of Ir^0 to $Ir^{\delta+}$ can be tuned by encapsulating bimetallic clusters within the zeolite micropores, thereby effectively regulating their redox properties. This is consistent with our previous finding on Ir clusters encapsulated within zeolite micropores[11]. Furthermore, NO molecule dissociation can be enhanced by electron-rich Ir^0 species through the electron donation from the metal center into the empty π^* orbital of NO[3], which is crucial for low-temperature catalytic performance. However, oxidized $Ir^{\delta+}$ species can promote selective NO adsorption in the presence of O_2 and even help maintain a balance between CO oxidation and NO reduction reactions in the presence of SO_2[11,31]. Moreover, the Ir 4f XPS signal intensity of Ir-Mo@Z5 is lower than that of Ir-Mo/Z5, indicating fewer metal species are dispersed on the external surface of Ir-Mo@Z5, which confirms that Ir-Mo bimetallic clusters are mainly confined within zeolite crystals via the one-step synthesis method. As shown in Supplementary Figure 7, compared with Ir@Z5, the binding energy of Ir $4f_{7/2}$ in Mo-modified Ir-Mo bimetallic cluster catalysts exhibits an obvious redshift of 0.45 eV toward lower binding energy. Given Ir's higher electronegativity compared to Mo, Mo tends to donate electrons in bimetallic clusters. After H_2 pretreatment at 200 °C, Mo species in Ir-Mo@Z5 and Ir-Mo/Z5 serve as electron donors, transferring partial electrons to Ir, thereby increasing the electron density at Ir sites. The electron-rich Ir^0 can

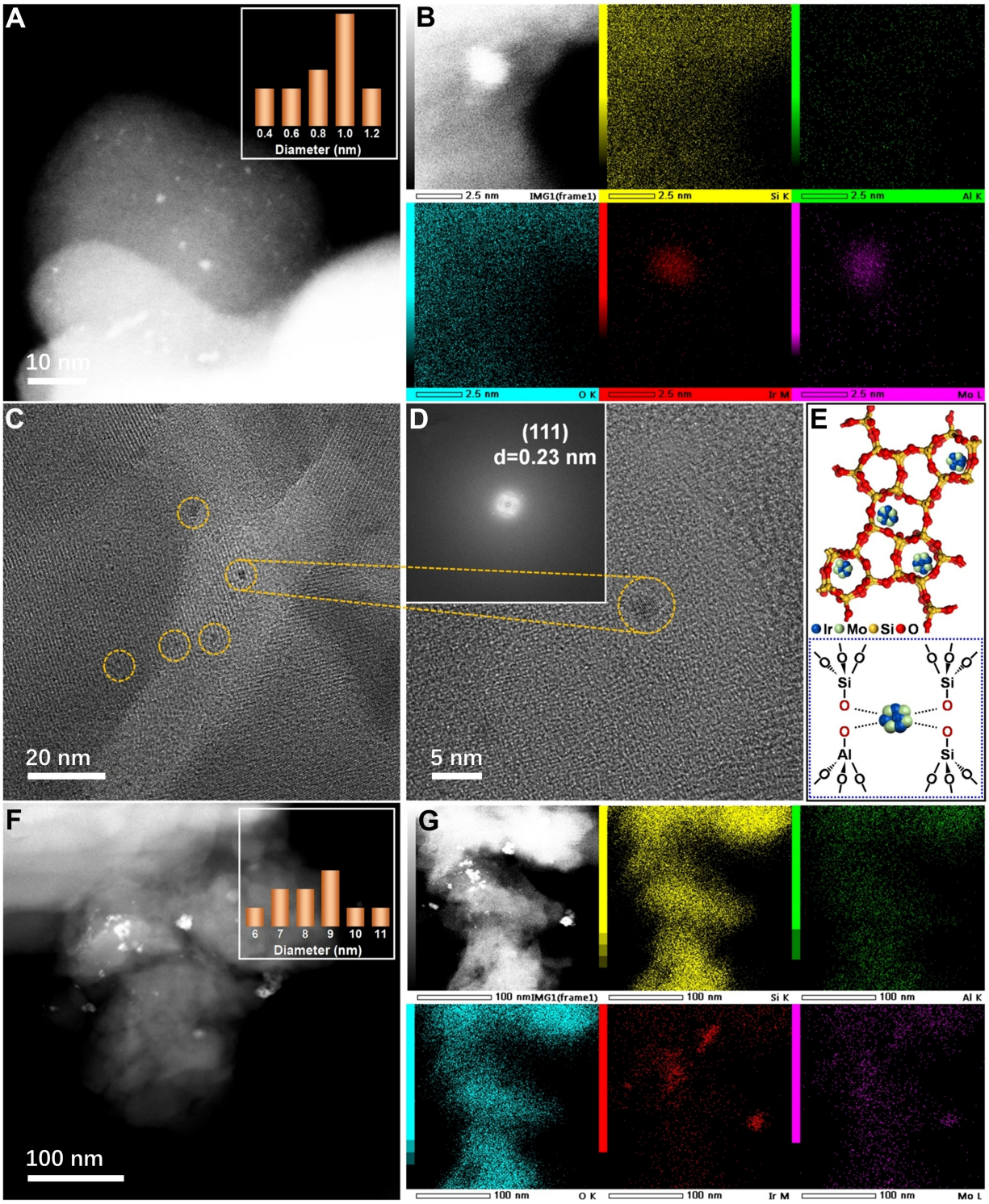

Figure 2. (A and B) TEM image and the corresponding EDS mapping images of Si, Al, O, Ir, Mo in Ir-Mo@Z5, (C and D) AC HAADF-STEM images of Ir-Mo@Z5, (E) structure diagram of Ir-Mo@Z5, and (F and G) TEM image and the corresponding EDS mapping images of Si, Al, O, Ir, Mo of Ir-Mo/Z5. TEM: Transmission electron microscopy; EDS: energy-dispersive X-ray spectroscopy; AC HAADF-STEM: aberration-corrected high-angle annular dark-field scanning transmission electron microscopy.

elongate the N–O bond and facilitate NO dissociation.

Mechanistic study

Temperature-programmed experiments were conducted to investigate the adsorption and desorption behaviors of NO and CO on the two catalysts. As shown in Figure 4A and B, two N_2O desorption

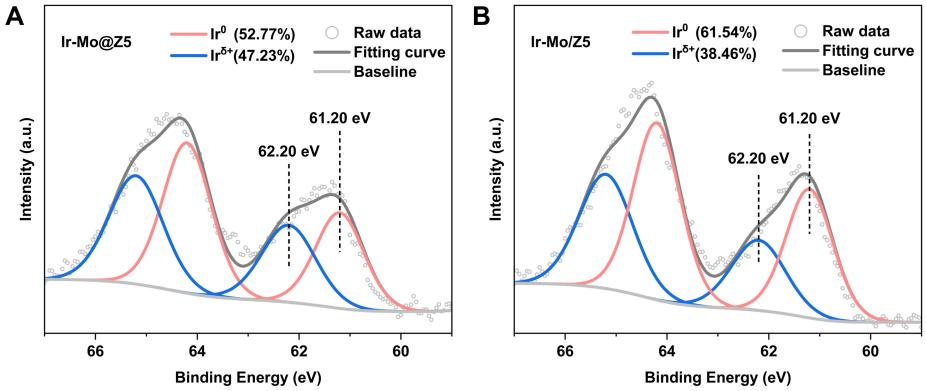

Figure 3. Ir 4f XPS spectra of (A) Ir-Mo@Z5 and (B) Ir-Mo/Z5 catalysts. XPS: X-ray photoelectron spectroscopy.

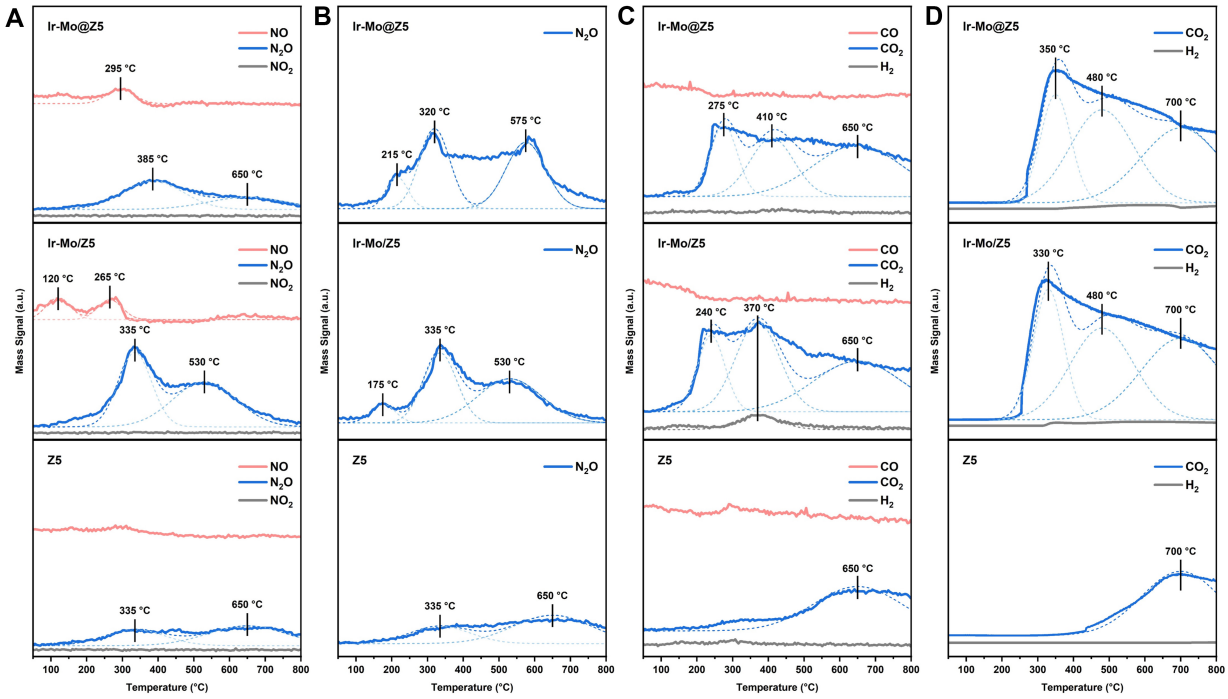

Figure 4. (A) NO-TPD profiles, (B) N_2O-TPD profiles, (C) CO-TPD profiles, and (D) CO-TPR profiles of Ir-Mo@Z5, Ir-Mo/Z5 catalysts and Z5 support. TPD: Temperature-programmed desorption; TPR: temperature-programmed reduction.

peaks were observed for the Z5 support at 335 and 650 °C in the NO-temperature-programmed desorption (NO-TPD) and N_2O-TPD profiles. This indicates that all NO molecules adsorbed on the Z5 support undergo a coupling-dissociation process[4,32]. The ONNO intermediate formed through coupling is prone to N–O bond cleavage, which is completed at temperatures below 335 °C. The NO-TPD results for the Ir-Mo@Z5 and Ir-Mo/Z5 catalysts also show NO desorption peaks. According to previous reports[13], these NO species are likely adsorbed and decomposed into nitrates. Compared with the three N_2O desorption peaks observed in the N_2O-TPD profiles (175, 335, and 530 °C), only two desorption peaks at 335 and 530 °C were observed in the NO-TPD profile of Ir-Mo/Z5. This indicates that the dissociation temperature of ONNO on Ir-Mo/Z5 is between 175 and 335 °C, whereas that on Ir-Mo@Z5 is between 320 and 385 °C. These results confirm that electron-rich Ir^0 species dominate the ONNO dissociation. Increasing the content of metallic Ir species in the catalyst is beneficial for intermediate conversion.

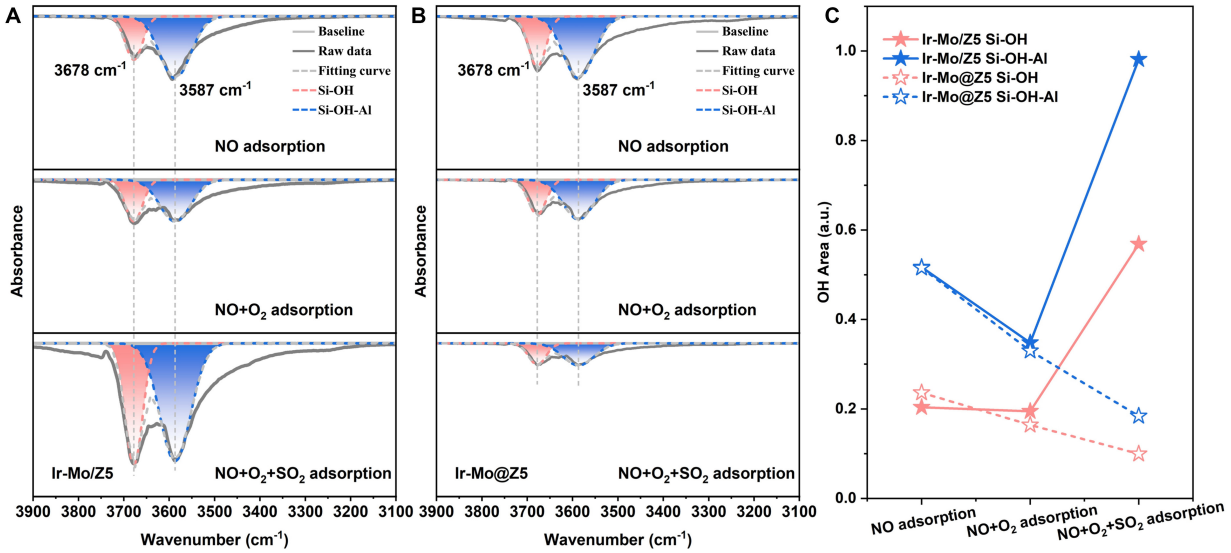

Figure 5. *In situ* DRIFTS results for pre-adsorbed NO, NO+O_2, or NO+O_2+SO_2 at 275 °C over (A) Ir-Mo/Z5 and (B) Ir-Mo@Z5 catalysts. Reaction conditions: [NO] = 400 ppm, [O_2] = 5%, [SO_2] = 200 ppm, and Ar balance; (C) Variation of Si-OH and Si-OH-Al peak areas with pre-adsorption on Ir-Mo/Z5 and Ir-Mo@Z5. *In situ* DRIFTS: *In situ* diffuse reflectance infrared Fourier transform spectroscopy.

As shown in Figure 4C, carbon dioxide (CO_2) is the only desorption product observed for the two catalysts and the Z5 support during programmed heating (after CO saturation); no significant CO desorption peak is detected, which is typically associated with the reaction between CO and lattice oxygen species. Compared with the CO_2 desorption peak observed on the Z5 surface at 650 °C, two additional desorption peaks appeared at lower temperatures for the Ir-Mo@Z5 and Ir-Mo/Z5 catalysts. Among them, the two CO_2 desorption peaks of Ir-Mo/Z5 occur at lower temperatures than those of Ir-Mo@Z5, indicating that the lattice oxygen activity of Ir-Mo/Z5 is superior to that of Ir-Mo@Z5. We propose that electrons are transferred from coordinated oxygen species to the Ir species, reducing the oxidized $Ir^{\delta+}$ species on Ir-Mo/Z5 to metallic Ir^0. This process facilitates oxygen-ion activation and vacancy formation to maintain charge balance[4,33], thereby explaining the lower activation temperature for CO oxidation on Ir-Mo/Z5. In addition, the simultaneous formation of CO_2 and H_2 at 370 °C on Ir-Mo/Z5 is observed, originating from the reaction between CO and surface -OH species ($2CO + 2OH \rightarrow 2CO_2 + H_2$)[34,35]. According to our previous report[11], Ir species loaded on the surface of Z5 usually occupy surface -OH groups[36], especially bridged silanol-aluminum groups (Si-OH-Al). Therefore, the larger bimetallic clusters on Ir-Mo/Z5 obtained via the conventional impregnation method imply fewer occupied -OH groups, which may be one of the reasons for the enhanced CO oxidation activity. Furthermore, Figure 4D shows the CO-TPR results. In general, the CO_2 desorption temperature corresponding to the reaction between gas-phase CO and lattice oxygen species is always higher than that for adsorbed CO on the two catalysts and the Z5 support, indicating that the Langmuir-Hinshelwood (L-H) mechanism occurs more readily at lower temperatures.

To investigate the effects of O_2 and SO_2 on reaction intermediates, NO, NO + O_2, or NO + O_2 + SO_2 were introduced over various catalysts at 275 °C. According to Wang *et al.*[37], the promotional effects of O_2 and SO_2 on the performance of Ir-based CO-SCR catalysts may be related to surface -OH groups. Once NO-adsorbed species occupy a portion of the catalyst surface -OH groups, the intensities of the negative -OH bands would decrease because fewer adsorption sites remain available for further adsorption. Figure 5A and B shows changes in the *in situ* DRIFTS spectra over the range of 3,100-3,900 cm^{-1} under different adsorption conditions. The absorption bands observed at 3,678 and 3,587 cm^{-1} are attributed to the stretching vibrations of isolated silanol groups (Si-OH) and the bridged silanol-aluminum groups (Si-OH-Al), respectively. After NO

introduction, the peak areas of Si-OH and Si-OH-Al decrease to different extents. To quantify the variations in the two -OH groups, Gaussian fitting was applied to deconvolute the infrared absorption bands, and the results are summarized in Figure 5C. The peak area of Si-OH-Al decreases more significantly after NO introduction, showing a reduction more than twice that of Si-OH on both Ir-Mo@Z5 and Ir-Mo/Z5 catalysts. This indicates that NO is more readily adsorbed on Si-OH-Al sites. However, once NO and O_2 were introduced simultaneously, the extent of Si-OH-Al consumption was significantly reduced, supporting the competitive adsorption between NO and O_2. Interestingly, the -OH groups on the two catalysts exhibited distinctly different trends after further SO_2 introduction. In general, the two types of -OH groups on the Ir-Mo/Z5 catalyst were significantly consumed, whereas those on the Ir-Mo@Z5 catalyst were largely preserved after SO_2 introduction. Wang *et al.*[37] reported that SO_2 is first oxidized to SO_3 on the Ir surface and subsequently forms sulfate species on -OH sites, thereby suppressing a series of side reactions in the presence of O_2. As shown in the SO_2-TPD profiles in Supplementary Figure 8, the SO_2 desorption amount is higher on supports with lower Si/Al ratios, providing direct evidence for SO_2 adsorption and activation by -OH groups. Our previous studies[22] also showed that SO_2 oxidation at Ir (111) sites is beneficial for suppressing the "ineffective reaction pathway" mediated by nitrate species in the presence of O_2. As mentioned earlier, more oxidized $Ir^{\delta+}$ species on Ir-Mo/Z5 are readily reduced to metallic Ir^0, facilitating oxygen ion activation and vacancy formation for charge balance maintenance, thereby resulting in higher lattice oxygen activity on Ir-Mo/Z5 than on Ir-Mo@Z5. Therefore, SO_2 is more readily oxidized on the Ir-Mo/Z5 catalyst, leading to greater consumption of -OH groups. These results clearly explain why the promotional effect of SO_2 is more pronounced over Ir-Mo/Z5 than over Ir-Mo@Z5, as shown in Figure 1 and Supplementary Figure 3.

The activity tests revealed that the mechanism by which SO_2 influences CO-SCR performance depends on the catalyst preparation method. The NO_x conversion over Ir-Mo@Z5 is higher than that over Ir-Mo/Z5 across the entire test temperature range, reaching a maximum of 62.4%. The one-step synthesis method yields small, uniform Ir-Mo bimetallic species confined within the zeolite interior, whereas the conventional impregnation method produces larger, unevenly distributed particles on the external surface. The formation of well-dispersed bimetallic structures is facilitated by appropriate reduction treatment. The confinement effect of zeolite micropores regulates the electronic state of the active sites, which is crucial for the adsorption and dissociation of NO molecules. Meanwhile, particles on the external surface favor surface oxygen activation and reactions with surface hydroxyl groups, thereby enhancing CO oxidation. These results demonstrate that the spatial distribution and electronic properties of the active sites can be rationally regulated through synthetic strategies, thereby governing the adsorption and reaction pathways of NO and CO.

To investigate the dynamic evolution of adsorbed species on the two catalysts, NO was first pre-adsorbed on the catalyst surface until saturation, followed by CO introduction to initiate the transient reaction [Supplementary Figure 9A and B]. Prominent characteristic adsorption peaks corresponding to ONNO (1,720-1,724 cm^{-1}) and N_2O_4 (1,683 cm^{-1}) were detected on both Ir-Mo@Z5 and Ir-Mo/Z5, with dimeric ONNO species serving as the dominant adsorbed intermediates[11]. After CO introduction, the intensity of the ONNO peak gradually decreased over time on both catalysts, confirming the synergistic catalytic effect of Ir and Mo sites in promoting ONNO dissociation. Notably, distinct adsorption peaks assigned to CO (2,057-2,063 cm^{-1}) and NO (1,830 cm^{-1}) adsorbed on metallic Ir^0 were observed over Ir-Mo/Z5, confirming the presence of Ir^0 species on this catalyst. In contrast, no obvious adsorption peaks associated with Ir^0 were detected on Ir-Mo@Z5. This strongly indicates that the one-step synthesis strategy effectively enhances the interaction between Ir and Mo within sub-nanoclusters and suppresses excessive reduction and aggregation of metallic species. To further explore the effect of O_2 on the CO-SCR reaction pathway, *in situ* DRIFTS experiments were conducted by introducing CO following the pre-adsorption of NO + O_2 [Supplementary Figure 9C and D]. Under aerobic conditions, the proportion of N_2O_4 species on Ir-Mo/Z5 increased markedly, whereas the formation of ONNO, a key low-temperature active intermediate, was significantly inhibited. By contrast,

ONNO remained the dominant NO adsorption species on Ir-Mo@Z5. This comparative result reveals that the strong bimetallic interaction within Ir-Mo sub-nanoclusters efficiently modulates the electronic structure of active sites and facilitates the directional conversion of NO into ONNO intermediates in the presence of O_2. The superior capability of Ir-Mo@Z5 to stably maintain ONNO formation and accelerate its dissociation and transformation under aerobic conditions accounts for its outstanding catalytic activity in the aerobic CO-SCR reactions. For both catalysts, NO first couples to form ONNO species, which subsequently dissociate. The difference in the ONNO dissociation temperature between the two catalysts is primarily determined by the electron-rich metallic Ir^0 species, and a higher Ir content facilitates intermediate conversion. For CO activation, it mainly reacts with lattice oxygen species to form CO_2. The catalyst prepared via the conventional impregnation method exhibits higher lattice-oxygen activity and, therefore, a lower CO oxidation temperature. This catalyst also provides more available surface hydroxyl groups, which further participate in CO oxidation.

In situ DRIFTS results indicate that although SO_2 exhibits similar promotional effects on NO_x conversion over the two catalysts, the underlying mechanisms differ. Undoubtedly, SO_2 promotes the actual efficiency of NO reduction to N_2. As we previously reported[22], this is attributed to the regulatory effect of SO_2 on the "ineffective reaction pathway" in the presence of O_2 with nitrate species as intermediates. More importantly, SO_2 effectively promotes NO adsorption onto catalysts prepared by conventional impregnation.

CONCLUSION

This work investigates a one-step-synthesized Ir-Mo@Z5 bimetallic cluster catalyst and systematically explores the role of surface hydroxyl groups in the SO_2-promoted CO-SCR reaction. The zeolite confinement effect enables the formation of highly dispersed Ir-Mo sub-nanoclusters (~1 nm), which preferentially occupy surface hydroxyl sites and suppress non-selective reactions between -OH groups and CO, thereby endowing Ir-Mo@Z5 with significantly enhanced NO_x conversion compared with the conventionally impregnated catalyst. *In situ* characterizations further verify that the consumption of Si-OH-Al by SO_2 effectively inhibits the nitrate-mediated non-productive reaction pathway under oxygen-containing conditions, revealing the intrinsic promotional mechanism of SO_2. Large-pore materials can be employed to confine the bimetallic clusters, allowing sufficient SO_2 diffusion into the pore channels and enabling reactions with surface hydroxyl sites occupied by Ir species, thereby suppressing non-productive reaction pathways and further enhancing CO-SCR catalytic performance. These aspects will be systematically investigated in future work.

DECLARATIONS

Authors' contributions

Data curation, validation, investigation, formal analysis, writing - original draft, writing - review and editing: Wang, Y.
Writing - review and editing, formal analysis: Ma, X.
Conceptualization, methodology: Liu, H.
Validation, formal analysis: Yuan, Y.
Methodology, formal analysis, writing - review and editing: Yang, Y.
Formal analysis, investigation: Zhang, Y.
Funding acquisition, validation, formal analysis, project administration, resources, writing - review and editing: Xu, W.
Resources, project administration, supervision: Zhu, T.

Availability of data and materials

The original contributions presented in this study are included in the article/Supplementary Materials. Further inquiries can be directed to the corresponding author.

AI and AI-assisted tools statement

Not applicable.

Financial support and sponsorship

This work was financially supported by the National Natural Science Foundation of China (Nos. 52400140 and 52470132).

Conflicts of interest

Xu, W. is an Editorial Board Member of the journal *Greenverse Science*. Xu, W. was not involved in any step of the editorial process, notably including reviewers' selection, manuscript handling, or decision-making. The other authors declare no

conflicts of interest.

Ethical approval and consent to participate

Not applicable.

Consent for publication

Not applicable.

Copyright

Supplementary Materials

Supplementary Materials

REFERENCES

1. Le Roy, E. J.; Wong, A. Y.; Eastham, S. D.; Fiore, A. M.; Selin, N. E. Impact of climate variability and change on the surface ozone response to NO_x emissions reductions. *Environ. Sci. Technol.* **2025**, *59*, 10422-33. DOI PubMed
2. Zhang, X.; Fung, J. C.; Lau, A. K.; Hossain, M. S.; Louie, P. K.; Huang, W. Air quality and synergistic health effects of ozone and nitrogen oxides in response to China's integrated air quality control policies during 2015-2019. *Chemosphere* **2021**, *268*, 129385. DOI PubMed
3. Jabłońska, M.; Palkovits, R. Copper based catalysts for the selective ammonia oxidation into nitrogen and water vapour - recent trends and open challenges. *Appl. Catal. B. Environ.* **2016**, *181*, 332-51. DOI
4. Liu, B.; Dai, G.; Wang, R.; et al. Co-based catalysts for the reduction of NO_x with CO via the regulation of geometric and electronic structure. *Coord. Chem. Rev.* **2025**, *532*, 216502. DOI
5. Li, S.; Chen, X.; Wang, F.; et al. Promotion effect of Ni doping on the oxygen resistance property of Fe/CeO_2 catalyst for CO-SCR reaction: activity test and mechanism investigation. *J. Hazard. Mater.* **2022**, *431*, 128622. DOI PubMed
6. Liu, J.; Burciaga, R.; Tang, S.; et al. Heterogeneous catalysis for the environment. *Innov. Mater.* **2024**, *2*, 100090. DOI
7. Li, R.; Liu, Z.; Li, J.; Wang, M.; Liu, Z. Advances in CO-SCR of NO_x in the presence of oxygen: strategies, reaction mechanisms, and key influencing factors. *Sep. Purif. Technol.* **2026**, *382*, 136086. DOI
8. Bai, Y.; Wu, Y.; Miao, C.; Wang, H.; Peng, Y.; Wu, Z. Sn-mediated regulation of the O_2 adsorption and activation capacity of the Ir/SAPO-34 catalyst: a key to boosting CO selective catalytic reduction of NO_x in O_2-enriched environments. *Environ. Sci. Technol.* **2025**, *59*, 26875-85. DOI PubMed
9. Haneda, M. Pusparatu, .; Kintaichi, Y.; et al. Promotional effect of SO_2 on the activity of Ir/SiO_2 for NO reduction with CO under oxygen-rich conditions. *J. Catal.* **2005**, *229*, 197-205. DOI
10. Sun, Y.; Wu, Y.; Bai, Y.; Wu, X.; Wang, H.; Wu, Z. High performance iridium loaded on natural halloysite nanotubes for CO-SCR reaction. *Fuel* **2024**, *357*, 129938. DOI
11. Chen, W.; Wang, Y.; Xu, W.; Li, C.; Yang, Y.; Zhu, T. Identifying spatially segregated Ir sites within ZSM-5 for enhanced redox cycle in NO_x reduction by CO. *Angew. Chem. Int. Ed.* **2025**, *64*, e202425312. DOI PubMed
12. Ji, Y.; Liu, S.; Zhu, H.; et al. Isolating contiguous Ir atoms and forming Ir-W intermetallics with negatively charged Ir for efficient NO reduction by CO. *Adv. Mater.* **2022**, *34*, 2205703. DOI PubMed
13. Wang, J.; Gao, F.; Yi, H.; et al. Strong Ir-W interaction boosts CO-SCR denitration over supported Ir-based catalysts and influential mechanism of oxygen. *Sep. Purif. Technol.* **2023**, *325*, 124684. DOI
14. Takahashi, A.; Nakamura, I.; Haneda, M.; Fujitani, T.; Hamada, H. Role of tungsten in promoting selective reduction of NO with CO over Ir/WO_3-SiO_2 catalysts. *Catal. Lett.* **2006**, *112*, 133-8. DOI
15. Kwon, D. W.; Park, K. H.; Hong, S. C. Enhancement of SCR activity and SO_2 resistance on VO_x/TiO_2 catalyst by addition of molybdenum. *Chem. Eng. J.* **2016**, *284*, 315-24. DOI
16. Li, Z.; Yang, J.; Zhou, Y.; et al. Influence of different preparation methods on the activity of Ce and Mo co-doped ZSM-5 catalysts for the selective catalytic reduction of NO_x by NH_3. *Environ. Sci. Pollut. Res.* **2020**, *27*, 40495-503. DOI PubMed
17. Li Z.; Huang W.; Xie K.C. Effect of Mo contents on properties of Mo/ZSM-5 zeolite catalyst for NO_x reduction. *J. Environ. Sci.* **2005**, *17*, 103-5. PubMed
18. Xie, Y.; Yang, X.; Li, Z.; et al. Competitive anchoring of Mo atoms induces Pt atoms agglomeration and enhanced electronic effects: elevated activity and selectivity for carbon disulfide hydrogenation. *Adv. Funct. Mater.* **2025**, *35*, 2505879. DOI
19. Fu, J.; Dong, J.; Si, R.; et al. Synergistic effects for enhanced catalysis in a dual single-atom catalyst. *ACS. Catal.* **2021**, *11*, 1952-61. DOI
20. Kato, A.; Matsuda, S.; Kamo, T.; Nakajima, F.; Kuroda, H.; Narita, T. Reaction between nitrogen oxide (NO_x) and ammonia on iron oxide-titanium oxide catalyst. *J. Phys. Chem.* **2002**, *85*, 4099-102. DOI
21. Bai, Y.; Gao, S.; Sun, Y.; et al. Insight into the mechanism of selective catalytic reduction of NO by CO over a bimetallic IrRu/ZSM-5 catalyst in the absence/presence of O_2 by isotopic $C^{13}O$ tracing methods. *Environ. Sci. Technol.* **2023**, *57*, 9105-14. DOI PubMed
22. Wang, Y.; Xu, W.; Liu, Z.; et al. Unveiling the mechanism of CO-SCR reaction over Ir/SiO_2 catalyst in the presence of multiple components (CO, O_2, SO_2). *Appl. Catal. B. Environ. Energy.* **2025**, *366*, 125066. DOI

23. He, J.; Chen, D.; Li, N.; et al. Controlled fabrication of mesoporous ZSM-5 zeolite-supported PdCu alloy nanoparticles for complete oxidation of toluene. *Appl. Catal. B:. Environ.* **2020**, *265*, 118560. DOI
24. Chen, G.; She, P.; Han, J.; et al. Structurally engineering multi-shell hollow zeolite single crystals via defect-directed oriented-kinetics transformation and their heterostructures for hydrodeoxygenation reaction. *Angew. Chem. Int. Ed.* **2025**, *64*, e202424690. DOI PubMed
25. Yang, L.; Liu, Q.; Han, R.; et al. Confinement and synergy effect of bimetallic Pt-Mn nanoparticles encapsulated in ZSM-5 zeolite with superior performance for acetone catalytic oxidation. *Appl. Catal. B. Environ.* **2022**, *309*, 121224. DOI
26. Cheng, K.; Van Der Wal, L. I.; Yoshida, H.; et al. Impact of the spatial organization of bifunctional metal-zeolite catalysts on the hydroisomerization of light alkanes. *Angew. Chem. Int. Ed.* **2020**, *59*, 3592-600. DOI PubMed
27. Wei, X.; Cheng, J.; Li, Y.; et al. Bimetallic clusters confined inside silicalite-1 for stable propane dehydrogenation. *Nano. Res.* **2023**, *16*, 10881-9. DOI
28. Liu, L.; Lopez-haro, M.; Lopes, C. W.; et al. Structural modulation and direct measurement of subnanometric bimetallic PtSn clusters confined in zeolites. *Nat. Catal.* **2020**, *3*, 628-38. DOI
29. Katrib, A.; Stanislaus, A.; Yousef, R. XPS investigations of metal - support interactions in Pt/SiO_2, Ir/SiO_2 and Ir/Al_2O_3 systems. *J. Mol. Struct.* **1985**, *129*, 151-63. DOI
30. Duan, X.; Sha, Q.; Li, P.; et al. Dynamic chloride ion adsorption on single iridium atom boosts seawater oxidation catalysis. *Nat. Commun.* **2024**, *15*, 1973. DOI PubMed PMC
31. Mingheng, Y.; Mulan, C.; Siyuan, X.; et al. Metal-support interaction governing Ir active-site properties for SO_2 reduction by CO. *Appl. Surf. Sci.* **2025**, *712*, 164150. DOI
32. Yan, X.; Liu, J.; Yang, Y.; Wang, Z.; Zheng, Y. A catalytic reaction scheme for NO reduction by CO over Mn-terminated $LaMnO_3$ perovskite: a DFT study. *Fuel. Process. Technol.* **2021**, *216*, 106798. DOI
33. Xu, X.; Liu, X.; Ma, L.; et al. Construction of surface synergetic oxygen vacancies on $CuMn_2O_4$ spinel for enhancing NO reduction with CO. *ACS. Catal.* **2024**, *14*, 3028-40. DOI
34. Sun, X.; Lin, J.; Wang, Y.; et al. Catalytically active Ir_0 species supported on Al_2O_3 for complete oxidation of formaldehyde at ambient temperature. *Appl. Catal. B. Environ. Energy.* **2020**, *268*, 118741. DOI
35. Li, Y.; Chen, X.; Wang, C.; Zhang, C.; He, H. Sodium enhances Ir/TiO_2 activity for catalytic oxidation of formaldehyde at ambient temperature. *ACS. Catal.* **2018**, *8*, 11377-85. DOI
36. Kong, F.; Nie, B.; Jiang, L.; et al. Progress in palladium-based bimetallic catalysts for lean methane combustion: towards harsh industrial applications. *Innov. Mater.* **2025**, *3*, 100116. DOI
37. Wang, J.; Gao, A.; Gao, F.; et al. The generation of sulfate species on Ir-based catalysts for boosting NO reduction with CO under the coexistence of O_2 and SO_2 atmosphere. *J. Colloid. Interface. Sci.* **2024**, *675*, 935-46. DOI PubMed